Inorganic Chemistry
Article

Inorg. Chem. **2009,** *48,* 4707–4713
DOI:10.1021/ic801779j

Three Lanthanum MOF Polymorphs: Insights into Kinetically and Thermodynamically Controlled Phases

Felipe Gándara,[†] Víctor A. de la Peña-O'Shea,[‡] Francesc Illas,[‖] Natalia Snejko,[†] David M. Proserpio,[§] Enrique Gutiérrez-Puebla,[†] and M. Angeles Monge*[,†]

[†]*Instituto de Ciencia de Materiales de Madrid, CSIC, Madrid, Spain,* [‡]*Instituto Madrileño de Estudios Avanzados en Energía (IMDEA Energía), and* [§]*Dipartimento di Chimica Strutturale e Stereochimica Inorganicaand Università di Milano, Milano, Italy, and* [‖]*Departament de Química Física & IQTCUB, Universidad de Barcelona, Barcelona, Spain*

Received September 17, 2008

RPF-4 is a family of polymeric frameworks prepared with rare-earth elements and the versatile ligand 4,4′-(hexafluoroisopropylidene)bis(benzoic acid). We have found that during the synthesis procedure up to three different polymorphs can be obtained. Their crystal structures are here presented. The three networks have unusual topologies, the three being uninodal penta-coordinated, two of them unknown up to now, and the other named **hxg-d-5-Imma**. They are here described and compared. DFT calculations of the relative energies for the three polymorphs show that the most often obtained structure is a metastable phase, which appears to be, next to others, thermodynamically more stable.

Introduction

The design and synthesis of microporous coordination networks with a novel structural topology obtained using polydentate ligands and a metal center have been of a great interest across disciplines because these metal-organic frameworks (MOFs) have been found to be a platform for immense potential applications[1−9] in gas storage, catalysis, magnetism, nonlinear optics, ion exchange reactions, separation processes, and so forth. Numerous studies have been presented of transition metal MOFs while the rare-earth (Ln) based MOFs are significantly less studied. However, the situation has been changing over the past few years due to the fact that Ln-based MOFs present a number of interesting opportunities with respect to their intriguing topologies and many interesting properties that may give rise to industrial applications from catalysis to optical materials.[10−12] In MOF materials, functionality is introduced from a cooperative influence of both inorganic species and organic linker molecules. This paper deals with the self-assembly of the lanthanide series with the 4,4′-(hexafluoroisopropylidene) bis(benzoic acid) ligand (H_2hfipbb). The long hydrophobic linker H_2hfipbb is a flexible molecule, which, being a dicarboxylate, establishes a bridge between different metal centers;[13−16] two novel frameworks have been recently obtained in our group, constructed from Zn[14] or In[16] and hfipbb. In these frameworks, the composition and shape of the intermediate part of the hfipbb^{2-} linker play an essential role in forming 3D and 2D polymeric structures of corresponding Zn and In MOFs. As a followup, we previously presented a short communication[17]

---

*To whom correspondence should be addressed. E-mail: amonge@icmm.csic.es.

(1) Sudic, A. C.; Cote, A. P.; Wong-Foy, A. G.; O'Keeffe, M.; Yaghi O. M. *Angew. Chem., Int. Ed.* **2006**, *45*, 2528.

(2) Kondo, A.; Noguchi, H.; Kajiro, H.; Carlucci, L.; Mercandelli, P.; Proserpio, D. M.; Tanaka, H.; Kaneko, K.; Kanoh, H. *J. Phys. Chem. B* **2006**, *110*, 25565.

(3) Rowsell, J. L. C.; Yaghi, O. M. *J. Am. Chem. Soc.* **2006**,, *128*, 1304.

(4) Jhung, S. H.; Lee, J.-H.; Cheetham, A. K.; Ferey, G.; Chang, J. S. *J. Catal.* **2006**, *239*, 97.

(5) Hong, M. *Cryst. Growth Des.* **2006**, *7*, 10.

(6) Vertova, A.; Cucchi, I.; Fermo, P.; Porta, F.; Proserpio, D. M.; Rondinini, S. *Electrochim. Acta* **2006**, *52*, 2603.

(7) Janiak, C. *Dalton Trans* **2003**, *14*, 2781.

(8) Braga, D.; Polito, M.; D'Addario, D.; Grepioni, F. *Cryst. Growth Des.* **2006**, *4*, 1109.

(9) Hyde, S. T.; Delgado-Friedrichs, O.; Ramsden, S. J.; Robins, V. *Solid State Sci.* **2006**, 740.

(10) Snejko, N.; Cascales, C.; Gómez-Lor, B.; Gutiérrez-Puebla, E.; Iglesias, M.; Ruiz-Valero, C.; Monge, M. A. *Chem. Commun.* **2002**, 1366.

(11) Gándara, F.; García-Cortés, A.; Cascales, C.; Gómez-Lor, B.; Gutiérrez-Puebla, E.; Iglesias, M.; Monge, A.; Snejko, N. *Inorg. Chem.* **2006**, *46*, 3475.

(12) Gándara, F.; Perles, J.; Snejko, N.; Iglesias, M.; Gómez-Lor, B.; Gutiérrez-Puebla, E.; Monge, M. A. *Angew. Chem.; Int. Ed.* **2006**, *45*, 7998.

(13) Pan, L.; Sander, M. B.; Huang, X; Li, J.; Smith, M.; Bitner, E.; Brockrath, B.; Johnson, K. J. *J. Am. Chem. Soc.* **2004**, *126*, 1308.

(14) Monge, A.; Snejko, N.; Gutiérrez-Puebla, E.; Medina, M.; Cascales, C; Ruiz-Valero, C.; Iglesias, M.; Gómez-Lor, B. *Chem. Commun.* **2005**, 1291.

(15) Pan, L.; Olson, D. H.; Ciemnolonski, L. R.; Heddy, R.; Li, J. *Angew. Chem., Int. Ed.* **2006**, *45*, 616.

(16) Gándara, F.; Gomez-Lor, B.; Gutiérrez-Puebla, E.; Iglesias, M.; Monge, M. A.; Proserpio, D. M.; Snejko, N. *Chem. Mater.* **2008**, *20*, 72.

(17) Gándara, F.; Andrés, A. d.; Gómez-Lor, B.; Gutiérrez-Puebla, E.; Iglesias, M.; Monge, M. A.; Proserpio, D. M.; Snejko, N. *Cryst. Growth Des.* **2008**, *8*(2), 378.

Table 1. Main Crystallographic and Refinement Data for the Three **La-RPF-4** Polymorphs

	RPF-4-α	**RPF-4-*β***	**RPF-4-*γ***
empirical formula	C_{51} H_{24} F_{18} La_2 O_{12}	C_{51} H_{24} F_{18} La_2 O_{12}	C_{51} H_{24} F_{18} La_2 O_{12}
fw	1448.52	1448.52	1448.52
cryst syst, space group	orthorhombic, *Pnan*	monoclinic, $P2_1/n$	orthorhombic, $C222_1$
unit cell dimensions	a = 7.7910(9) Å α = 90°	a = 7.5600(3) Å α = 90°	a = 7.7910(9) Å α = 90°
	b = 21.372(3) Å β = 90°	b = 25.8914(1) Å β = 90.8540(1)°	b = 21.372(3) Å β = 90°
	c = 36.997(3) Å γ = 90°	c = 29.6752(1) Å γ = 90°	c = 36.997(3) Å γ = 90°
volume	6160.2(13) Å^3	5583.6(4) Å^3	5235.7(10) Å^3
Z, calculated density	4, 1.562 Mg/m^3	4, 1.723 Mg/m^3	4, 1.838 Mg/m^3
abs coeff	1.475 mm^{-1}	1.628 mm^{-1}	1.736 mm^{-1}
F(000)	2808	2808	2808
cryst size	0.06 × 0.04 × 0.02 mm	0.20 × 0.10 × 0.06 mm	0.12 × 0.10 × 0.07
Θ range for data collection	1.10−28.62°	1.07−25.68°	1.31−26.48°
limiting indices	$0 \leq h \leq 10$	$-9 \leq h \leq 9$	$-9 \leq h \leq 9$
	$0 \leq k \leq 28$	$-30 \leq k \leq 30$	$-38 \leq k \leq 38$
	$0 \leq l \leq 48$	$-35 \leq l \leq 36$	$-27 \leq l \leq 28$
reflns collected/unique	22622/7622	36747/10356	21371/5360
Absorption correction	semiempirical from equivalents	semiempirical from equivalents	semiempirical from equivalents
max. and min. transmission	0.9711 and 0.9167	0.9087 and 0.7367	0.8882 and 0.8188
refinement method	full-matrix least-squares on F^2	full-matrix least-squares on F^2	full-matrix least-squares on F^2
Data/restraints/parameters	22866/160/293	10356/355/748	5360/0/376
goodness-of-fit on F^2	0.863	1.130	1.264
final R indices [$I > 2\sigma(I)$]	$R_1 = 0.1385$, $wR_2 = 0.2388$	$R_1 = 0.0892$, $wR_2 = 0.1691$	$R_1 = 0.0898$, $wR_2 = 0.2019$
R indices (all data)	$R_1 = 0.4358$, $wR_2 = 0.3620$	$R_1 = 0.1547$, $wR_2 = 0.1979$	$R_1 = 0.0973$, $wR_2 = 0.2114$
largest diff. peak and hole	2.454 and −3.197 e A^{-3}	0.946 and −2.283 e A^{-3}	2.050 and −5.090 e A^{-3}

reporting a series of novel isostructural lanthanide MOFs with the same ligand, called RPF-4, showing excellent optical properties, as well as catalytic activity. In this paper, we report the extended data of the synthesis study of the Ln−hfipbb system. During the synthesis procedure, up to three different polymorphs have been identified, named α, β, and γ, and their crystal structures determined. Polymorphism is an interesting and well-known phenomenon; there exist numerous examples of compounds with more than one crystalline phase, being of special interest those of pharmacologically important molecules.[18] In the case of MOFs, however, there are not too many examples of real polymorphism.[19] In the current work, a topological analysis for the three new polymorphs is now reported, together with DFT calculations with a comparison of the relative energy for the three networks.

Experimental Section

All chemicals were of reagent grade and were used as commercially obtained without further purification. The IR spectrum was recorded from KBr pellets in the range 4000−400 cm^{-1} on a Perkin-Elmer spectrometer. The powder X-ray diffraction was performed with a Bruker D8 difractometer.

General Synthesis Procedure. During the first attempts to synthesize the new Ln^{3+}-based materials with the ligand H_2hfipbb, a mixture of phases with different crystal structures was obtained. Only after determining their crystal structures did the same formula, $Ln_2(hfipbb)_3$, for the three phases result, three polymorphs for the RPF-4 family, that we call **α**, ***β***, and ***γ***. By adjusting the synthesis conditions, we could get the materials as pure phases. The materials of the new family of the rare-earth polymeric framework, **RPF-4-α**, were synthesized via hydrothermal reactions of R(III) (R = Y, La, Ce, Pr, Nd, Sm, Eu, Gd, Tb, Dy, Ho, Er, Yb) salts with H_2hfipbb in a mixture of solvents. Typically, a mixture of $Ln(NO_3)_3$ (0.1 mmol), H_2hfipbb acid ($C_{17}H_{10}F_6O_4$; 0.15 mmol), ethyleneglycol (2 mL), ethylenediamine (0,2 mL), and H_2O (12 mL) was put in a Teflon-lined acid digestion bomb (internal volume of 43 mL) and heated at 170 °C for 2 days, followed by cooling to room temperature. The crystalline products (the color of the crystalline powder depends on the metal used) were collected after washing with H_2O (3 × 20 mL) and acetone (2 × 10 mL). Yields were 60−70%. The pure **RPF-4-*β*** (R = La) was obtained from a mixture of $La(NO_3)_3$ (0.1 mmol), H_2hfipbb acid (0.15 mmol), triethylamine (0.3 mL), and H_2O (5 mL). Heating this mixture in a Teflon-lined acid digestion bomb at 170 °C for 5 days, followed by cooling to room temperature, resulted in pure white crystalline product **La-RPF-4-*β***. The **RPF-4-*γ*** (R = La) polymeric framework was obtained from a mixture of $La(NO_3)_3$ (0.1 mmol), H_2hfipbb acid (0.15 mmol), 4,4-bipyridyl (0.1 mmol), and H_2O (6 mL). Heating this mixture in a Teflon-lined acid digestion bomb at 180 °C for 4 days, followed by cooling to room temperature, resulted in a mixture of crystalline powder **La-RPF-4-α** and colorless large crystals of **La-RPF-4-*γ***. All attempts to obtain **La-RPF-4-*γ*** as a pure phase were not successful. It is worth noting that, if we use the synthesis conditions that lead to the obtaining of **RPF-4-α**, but augmenting the time of the reaction (up to 5 days), a mixture of **RPF-4-α** and **RPF-4-*β*** is obtained.

Crystal Structure Determination. The data collection of **La-RPF-4-α** was reported in ref 17. Main crystallographic and refinement data are given in Table 1, for comparison with those of **La-RPF-4-*β*** and **La-RPF-4-*γ***. For **La-RPF-4-*β*** and **La-RPF-4-*γ***, the data were collected at room temperature, on a SMART-CCD Bruker diffractometer, with Mo Kα radiation (λ = 0.71073 Å). Data were collected over a hemisphere of the reciprocal space through a combination of sets of exposures. Each exposure of 20 s covered 0.3° in ϕ. Unit cell dimensions were determined by a least-squares fit of 60 reflections with $I > 20\sigma(I)$. The structures were solved by direct methods. The final cycles of refinement were carried out by full-matrix least-squares analyses with anisotropic thermal parameters for all non-hydrogen atoms. Hydrogen atoms were geometrically

---

[18] (a) Munshi, P.; Skelton, B. W.; McKinnon, J. J.; Spackman, M. A. *CrystEngComm* **2008**, *10*, 197. (b) Barsky, I.; Bernstein, J. *CrystEngComm* **2008**, *10*, 669.(c) Kitamura, M. *Cryst. Growth Des.* **2004**, *4*, 1153. (d) Herbstein, F. H. *Cryst. Growth Des* **2004**, *4*, 1419.

[19] (a) Chen, B.; Fronczek, F. R.; Maverick, A. W. *Chem. Commun.* **2003**, 2166. (b) Chen, B.; Ockwig, N. W.; Fronczek, F. R.; Contreras, D. S.; Yaghi, O. M. *Inorg. Chem.* **2005**, *44*, 181. (c) Li, Z.-G.; Wang, G.-H.; Jia H.-Q.; Hu, N.-H.; Xu, J.-W. *CrystEngComm* **2007**, *9*, 882.

located. Calculations were carried out with SMART software for data collection and data reduction and SHELXTL.[20]

Computational Details. Density functional plane-wave calculations have been carried out with the help of the VASP code[21,22] for the three lanthanum MOFs. There are 428 atoms in the unit cell ($C_{204}H_{96}F_{72}La_8O_{48}$). The energy is calculated employing the generalized gradient approximation, in particular, the exchange and correlation functional of Perdew and Wang (PW91).[23,24] The density was expanded in a plane wave basis set, whereas the effect of the inner cores was taken into account through the projected augmented plane wave method.[25,26] The cutoff for kinetic energy of the plane waves has been set to 415 eV throughout, which ensures a total energy convergence of better than 10^{-4} eV. A Gaussian smearing technique with a 0.2 eV width has been applied to enhance convergence, but all energies presented have been obtained by extrapolating to zero smearing (0 K). Geometry optimization on selected starting geometries obtained from single-crystal X-ray diffraction vh(see corresponding experimental details) was carried out using a gradient-conjugate method until forces on all atoms were less than 0.3 eV/nm. All calculations have been carried out on a parallel CESCA supercomputer.

Results and Discussion

The **Ln_2(hfipbb)$_3$** MOF presents three different polymorphs, named **α**, ***β***, and *γ*. The polymorphs **α** and ***β*** tend to appear together in most of the synthesis experiments. Only after a fine adjustment of the hydrothermal conditions (see the Experimental Section) were these two polymorphs obtained as pure phases. The polymorph **La-RPF-4-*γ*** could not be obtained as a pure phase. Crystals of the monoclinic polymorph **La-RPF-4-*β*** (isostructural with one of Eu[27] recently reported) and orthorhombic polymorph **La-RPF-4-*γ*** are quite good, and the structures can be easily determined. The orthorhombic polymorph **La-RPF-4-α**, however, is only obtained as fine crystalline powders, with few small twinned crystals in some cases. Powder diffraction patterns of this orthorhombic phase show that the compounds for all rare-earth elements are isostructural and quite similar to that of our Zn(hfipbb) compound previously reported[10] and also to that, later reported,[27] with cell parameters $a = b = 21.32$ Å, $c = 7.71$ Å, and $V = 3009.4$ Å^3.

Only small twinned crystals apt for the structure determination were obtained in the case of the lanthanum compound. The careful analyses of the diffraction pattern gave us another hexagonal cell unit with double *a* and *b* and quadruple volume. Only after thorough study of the data could we solve the twin by applying the matrix

$$\begin{vmatrix} 0 & 0 & 1 \\ 1 & 0 & 0 \\ 1 & 2 & 0 \end{vmatrix}$$

to a hexagonal cell quite similar to that of the Zn compound, which drove us to the final orthorhombic cell. The structure could then be solved in the space group *Pnan* ($a = 7.79$ Å, $b = 21.37$ Å, $c = 37.00$ Å, $V = 6160.2$ Å^3). Subsequently, the presence of three orthorhombic components in the twinned crystal was confirmed and refined to a composition of 47:29:24%. The structure solution was also employed to refine the obtained bulk samples of the compounds with the Rietveld refinement of the X-ray synchrotron data for La[17] and with laboratory X-ray data for the whole family (Figure 1).

Upon determining the crystal structure, the composition of the three compounds was found to be [$La_2(C_{17}H_8F_6O_4)_3$]. The La ion is always nine-coordinated (Table 2). In **La-RPF4-α** and **La-RPF4-*γ***, the asymmetric unit comprises one-half of the formula, while in **La-RPF4-*β***, there are two independent La atoms, and therefore one molecular formula per unit cell. In the three structures, chains of La atoms are formed along the *a* axis via the μ_2 oxygen atoms (Figure 2, bottom). The anions link these chains, giving rise to 3D structures.

In the case of **RPF-4-α**, a channelled structure with three parallel tunnels down the *a* axis is formed. Two of the channels are square-shaped (A and B), and one is hexagonal (C; Figure 3). All of these channels are empty and have a free void cylindrical space with a window of diameters 5.2−5.5 Å, as computed by Platon[28] (cavity routine). Although the structure looks quite similar to that of the previously reported zinc compound,[10] it has a different topology. The network of the Zn compound is uninodal four-connected (short symbol ($6^5.8$)), while in the La compound, the net is uninodal five-connected. Each node/La ion is directly connected to two other La ions of the same chain via bridging carboxylate oxygen atoms of the ligand, and also to three other La ions from different chains via the whole ligand as linkers. The result is a net with a point symbol of ($4^2.6^8$) (this net has been recently found in a search for net relations[29,30] and named **hxg-d-5-*Imma***[21]); topological analysis was performed using TOPOS.[31,32] In contrast to what happened for the Zn compound, where all of the metallic chains are connected through the ligand anions in a crossing way, in the Ln compounds, these connections are established in two different manners: two of them crossing (for the channels of A-type) and one parallel (for the channels of B-type) (Figure 3, right). The different distribution of the A and B channels breaks the hexagonal symmetry and explains the preference for triple twins. Due to the bent geometry of the ligand, its central atom being a sp^3 carbon, the fluorine atoms are all pointing into the C hexagonal channels. Consequently, the walls of the hexagonal tunnel are formed by CF_3 groups, giving rise to hydrophobic fluoro-lined Teflon-like channels.

The two other polymorphs (Figure 4) exhibit a more dense structure, with smaller cell volumes than the first structure: **RPF-4-α** has a cell volume of 6160.2(13) Å^3, with

---

(20) *SMART System*, V.5.04; *SHELXTL*, V.5.1; Bruker-Siemens Analytical X-ray Instrument Inc.: Madison; WI; 1998.

(21) Kresse, G.; Furthmüller, J. *Comput. Mater. Sci.* **1996**, *6*, 15.

(22) Kresse, G.; Hafner, J. *Phys. Rev. B* **1993**, *47*, 558.

(23) Perdew, J. P.; Wang, Y. *Phys. Rev. B* **1992**, *45*, 13244.

(24) Perdew, J. P.; Chevary, J. A.; Vosko, S. H.; Jackson, K. A; Pederson, M. R.; Singh, D. J.; Fiolhais, C. *Phys. Rev. B* **1992**, *46*, 6671.

(25) Blöchl, P. E. *Phys. Rev. B* **1994**, *50*, 17953.

(26) Kresse, G.; Joubert, D. *Phys. Rev. B* **1999**,, *59*, 1758.

(27) Harbuzaru, B. V.; Corma, A.; Rey, F.; Atienzar, P.; Jordá, J. L.; García, H.; Ananias, D.; Carlos, L. D.; Rocha, J. *Angew. Chem., Int. Ed.* **2008**, *47*(6), 1080.

(28) Spek, A. L. *PLATON*; Utrecht University: Utrecht, The Netherlands, 2007.

(29) Blatov, V. A. *Acta Crystallogr., Sect. A* **2007**, *63*, 329.

(30) VS [$4.4.6.6.6_2.6_2.6_4.6_4.6_4.6_6$] and coordination sequence (5;18;45;82;128;190;262;340;437;544).

(31) Blatov, V. A. *IUCr Compcomm Newsletter* 2006, 7, 4. http://www.topos.ssu.samara.ru (accessed Apr 2009).

(32) Blatov, V. A.; Carlucci, L.; Ciani, G.; Proserpio, D. M. *CrystEngComm.* **2004**, *6*, 377.

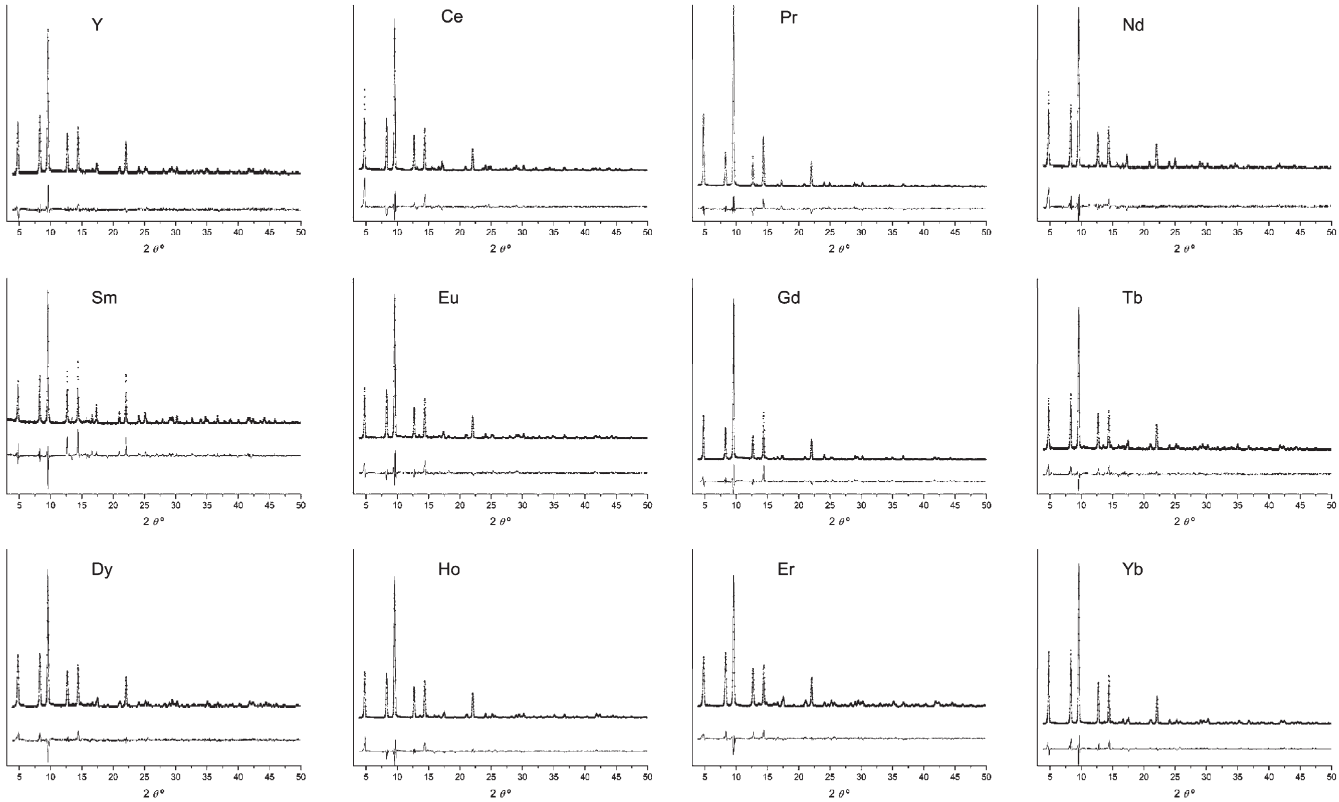

Figure 1. Rietveld refinement of the **Ln-RPF-4-α** structure showing experimental (dot), simulated (line), and difference patterns.

Table 2. Interatomic Distances in the Coordination Sphere of the Three **La-RPF-4** Polymorphs

RPF-4-α[a]		RPF-4-β[b]				RPF-4-γ[c]	
La(1)−O(1)	2.443(12)	La(1)−O(12)#a	2.473(7)	La(2)−O(10)	2.470(7)	La(1)−O(6)#b	2.505(10)
La(1)−O(6)#a	2.443(12)	La(1)−O(6)	2.491(7)	La(2)−O(8)#b	2.487(8)	La(1)−O(4)#a	2.505(11)
La(1)−O(2)#a	2.456(14)	La(1)−O(9)	2.499(8)	La(2)−O(11)	2.500(8)	La(1)−O(1)	2.521(10)
La(1)−O(4)	2.467(11)	La(1)−O(1)	2.501(8)	La(2)−O(2)	2.536(7)	La(1)−O(3)	2.533(11)
La(1)−O(3)#b	2.471(12)	La(1)−O(4)#a	2.501(7)	La(2)−O(3)	2.539(7)	La(1)−O(2)#b	2.545(12)
La(1)−O(5)	2.560(12)	La(1)−O(7)	2.526(8)	La(2)−O(5)	2.568(8)	La(1)−O(5)	2.578(10)
La(1)−O(6)	2.668(11)	La(1)−O(10)	2.622(7)	La(2)−O(4)	2.612(7)	La(1)−O(6)	2.637(10)
La(1)−O(2)	2.712(13)	La(1)−O(2)	2.658(7)	La(2)−O(12)	2.616(7)	La(1)−O(1)#b	2.675(11)
La(1)−O(3)	2.769(11)	La(1)−O(8)	2.803(7)	La(2)−O(6)	2.677(7)	La(1)−O(4)	2.878(11)

[a] Symmetry transformations used to generate equivalent atoms. #a: $x - 1/2, -y + 1, z$. #b: $x + 1/2, -y + 1, z$. [b] Symmetry transformations used to generate equivalent atoms. #a: $x + 1, y, z$. #b: $x - 1, y, z$. [c] Symmetry transformations used to generate equivalent atoms. #a: $x - 1/2, -y + 1/2, -z$. #b: $x + 1/2, -y + 1/2, -z$.

a 23.8% of free volume, while those for **RPF-4-*β*** and **RPF-4-*γ*** are 5583.6(4) Å^3 and 5235.7(10) Å^3, with a free volume of 15.9% and 3.7%. The networks of **RPF-4-*β*** and **RPF-4-*γ*** can also be simplified as rods of La atoms, running along the *a* axis. The ligand is then considered as a linker between two La nodes from different chains. Opposite of **RPF-4-α**, where all of the interchain connections are made through two linkers, above and below the chains, in **RPF-4-*β*** and **RPF-4-*γ***, there is a connection between chains which is made only by one ligand: in **RPF-4-*β***, along the *b* axis and, in **RPF-4-*γ***, along the *c* axis. The joining along the remaining direction is made by two linkers, above and below the chains. However, this connection is different in each case: in **RPF-4-*β***, they are all made in a parallel mode, with no edge-crossing presence, while in **RPF-4-*γ***, they are all arranged in an edge-crossing manner (Figure 2, top). As a result, these two networks, also uninodal pentacoordinated, have different unprecedented topologies[33] with a point (Schläfli) symbol of ($4^4.6^4.8^2$) for **RPF-4-*β*** and (6^{10}) for **RPF-4-*γ***. Notwithstanding that the infinite chains give simple rod packings for all three compounds (**α**, hexagonal type I, ***β*** and ***γ*** square type II),[34] the bent ligands give a final topology more complex than the simplest possible five-connected bnn and six-connected pcu nets derived from two such kinds of rod packings.

---

(33) RPF-4-*β*: vertex symbol, [$4.4.4.4.6.6.6.8_{13}.8_{13}.*$]; coordination sequence, (5;16;45;96;169;264;377;508;657;824). RPF-4-*γ*: vertex symbol, [$6_3.6_3.6_3.6_3.6_3.6_3.6_3.6_3.6_3.6_3$]; coordination sequence, (5;20;52;112;188; 284;391;516;653;808). The maximum symmetry embedding of the nets (the "ideal nets") observed in the polymorphs α and *γ* present edge-crossings similar to the 3D net in the Zn derivative (ref 10) and the two-periodic 3D in the In layers (ref 16). Such crossings are avoided in the real structures due to the flexible ligands that bend over.

(34) Rosi, N. L.; Kim, J.; Eddaoudi, M.; Chen, B.; O'Keeffe, M.; Yaghi, O. M. *J. Am. Chem. Soc.* **2005**, *127*, 1504.

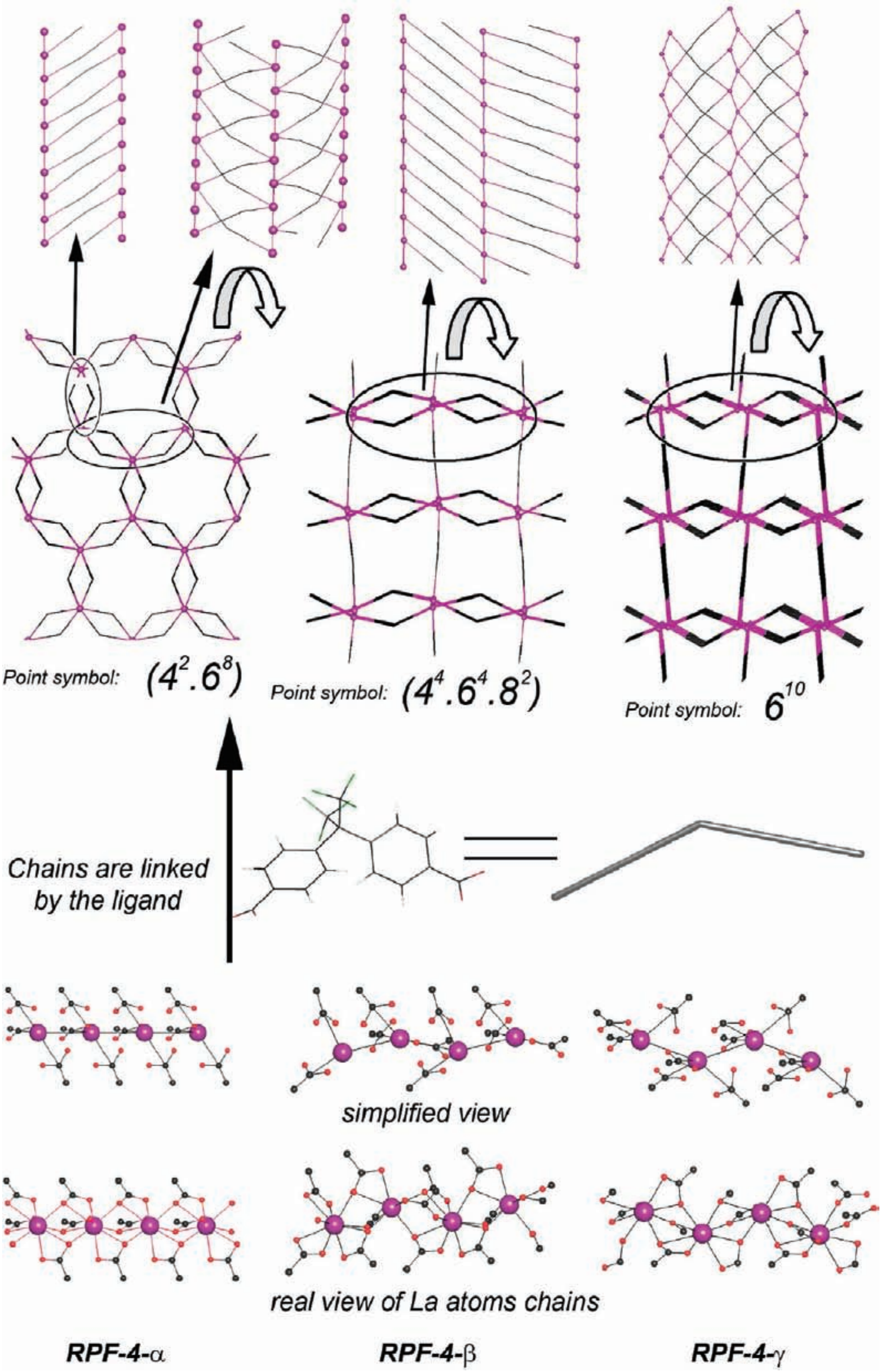

Figure 2. Topological analysis of the three **RPF-4** polymorphs.

The three nets can also be compared in other ways, describing layers of square (more or less deformed) channels, parallel to the ab plane for the α and the *β*, and to the ac plane in the case of *γ* polymorph (figure 5). Thus, in both α and *γ* polymorphs, the layers are ligand-crossed. In the *γ* polymorph, the layers stack on 010 joined by the remaining ligand; in the α polymorph, the layers are undulated, stacking on 001 and joined by the no crossing ligands. Actually, in this α polymorph, we can also find the undulated layers containing the square channels by rotating the cell ±60° over the *a* axis, but then the distribution of the crossing and no crossing ligands is different, which may be the cause of the triple twinning in this structure.

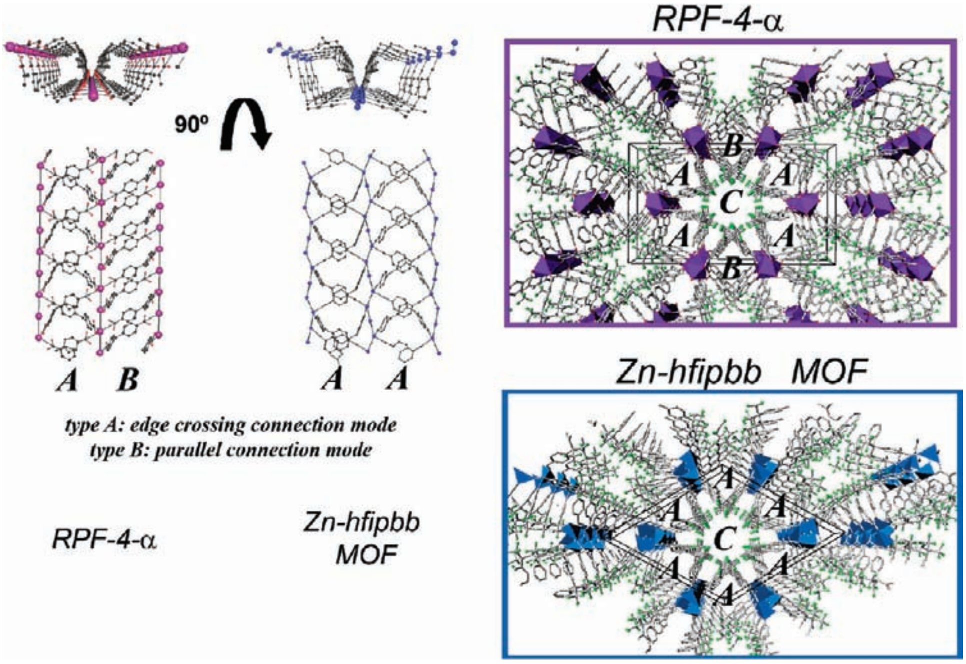

Figure 3. Comparison between **RPF-4-α** and Zn-hfipbb MOFs.

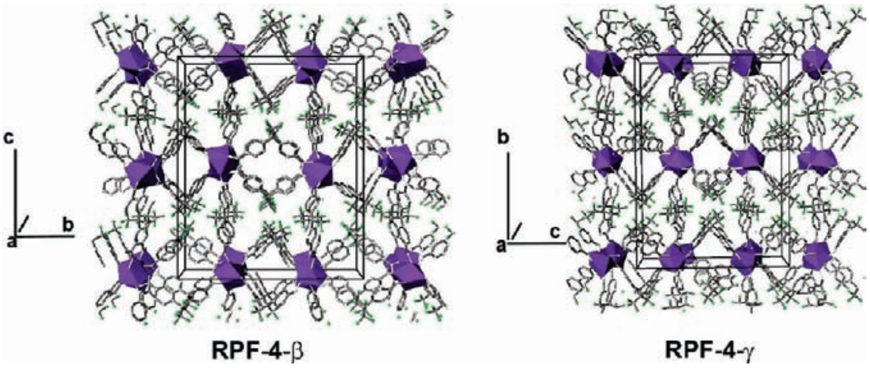

Figure 4. A view of the two new La-hfipbb polymorphs.

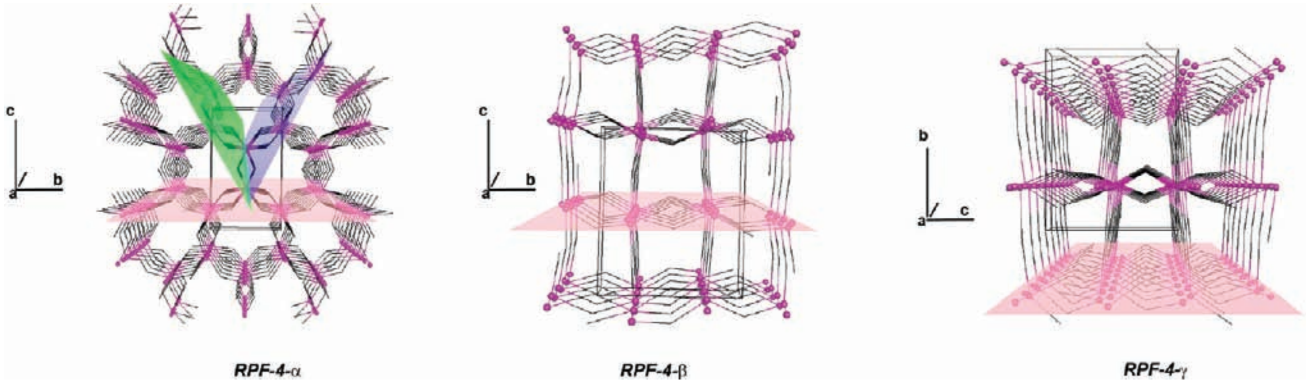

Figure 5. Comparison of the three simplified networks. Layers containing the La atoms and the square channels are represented. In the case of the α polymorph, the two other possible orientations for these planes, the cause of the twinning, are shown with different colors.

Conformational and energetic DFT-based calculations are commonly used in several chemistry fields as organic and inorganic systems. In the case of MOFs, the majority of works that raise these studies are performed using molecular mechanics calculations, due to the size of these systems. Only a limited number of studies use an ab initio DFT methodology. DFT plane wave periodic calculations have been extensively performed in solid-state chemistry (perovskites and catalysts, among others) because they offer a better interpretation of periodic solid frameworks. However, these

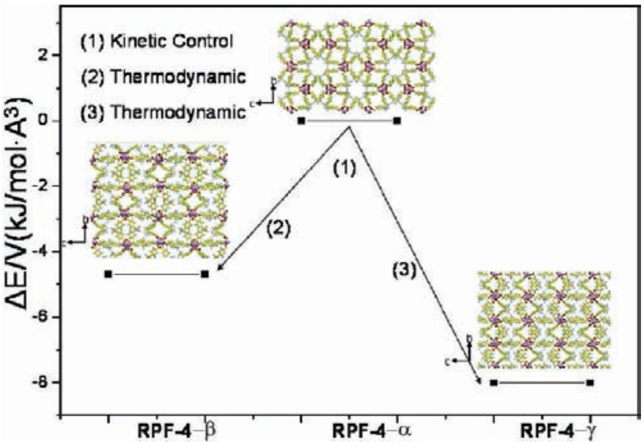

Figure 6. Energy gap diagram of different polymorphs, obtained by DFT calculations.

studies are much less applied to MOF materials, although some groups have begun to use these kinds of methods.[35]

A study of the relative energies of the three polymorphs in the La–hfippb **RPF-4** system has also been carried out. The geometry optimization always converged to a stable structure with the same topology that the experimental structures exhibited as obtained by X-ray diffraction, even though no symmetry constraints were imposed. As observed in Figure 6 and taking into account the experimental results, the α polymorph is a metastable structure kinetically controlled. The changes of the synthesis conditions give rise to the other two different polymorphic phases (that often are observed together with α). The DFT calculation shows that these crystal polymorphs (*β* and *γ*) are more stable than α, and therefore they are thermodynamically controlled.

The solution-phase synthesis, especially hydro- or solvothermal synthesis, is often controlled kinetically, giving rise to the growth of metastable phases. Thus, the optimization of the synthesis conditions is critical and can play a crucial role in the design of thermodynamically unstable unknown structures with interesting properties that are technologically useful.

Conclusions

In summary, up to three polymorphs can be obtained in the La–hfipbb system. The crystal structures for the three of them have been solved and refined, including one with a triple twinned structure. The structural and topological analysis here reported demonstrate that the use of a versatile ligand such as hfipbb can lead to the formation of different networks with different features, some of them with very interesting properties, as it has been already reported.[17] In addition, the energetic calculations carried out for the three compounds demonstrate that the most frequently found structure is a metastable phase, which appears together with others thermodynamically more stable. The formation of this metastable phase is controlled by kinetic factors, and it can be obtained purely with a fine control of the synthesis conditions.

Acknowledgment. F.G. acknowledges an FPI fellowship from Ministerio de Educación y Ciencia (MEC) and Fondo Social Europeo from the EU. This work has been supported by the Spanish MCYT Project Mat 2007-60822, CTQ 2007-28909-E/BQU, and Consolider-Ingenio CSD2006-2001. Allocation of computational time on the CESCA supercomputer of the Centre de Supercomputació de Catalunya is acknowledged.

Supporting Information Available: X-ray crystallographic files in CIF format. This material is available free of charge via the Internet at http://pubs.acs.org.

---

(35) (a) Keskin, S.; Liu, J.; Rankin, R. V.; Karl Jhonson, J.; Sholl, D. S. *Ind. Eng. Chem. Res.* **2009**, *48*, 2355 and references therein. (b) Coombes D. S.; Cora, F.; Mellot-Draznieks, C.; Bell, R. G. *J. Phys. Chem. C* **2009**, *113*, 544.(c) Sillar, K.; Hofmann, A.; Sauer, J. *J. Am. Chem. Soc.* 2009, DOI: 10.1021/ja8099079.